Quantifying Bird Density During Migratory Stopover Using Weather Surveillance Radar

Jeffrey J. Buler and Robert H. Diehl

***Abstract*—Increasingly, data from weather surveillance radars are being used by biologists investigating the ecology and behavior of birds, insects, and bats in the aerosphere. Unfortunately, these radars quantify echoes caused by layered biological targets such as migrating birds in a manner that introduces bias in radar measures. We investigated the performance of a bias-adjustment algorithm that adjusts radar measures for vertical variation of reflectivity, nonstandard beam refraction, and spatial displacement of radar targets. We evaluated the efficacies of four variations of this algorithm by their ability to increase correspondence between radar reflectivity measured at two weather radar sites and the ground density of migrating birds measured during two autumn seasons and two spring seasons among 24 hardwood forest sites along the northern coast of the Gulf of Mexico. The algorithm integrated close-range reflectivity data from the five lowest elevation angle sweeps to derive high-resolution vertical profiles of reflectivity (VPRs) that closely corresponded to the observed vertical target density profiles based on a vertically oriented portable radar. The radar reflectivity of birds aloft near the onset of migratory flight was positively correlated with the bird density on the ground. All four radar data adjustment schemes that we tested produced significant improvement in the accuracy of bird density estimates relative to unadjusted radar data. In general, adjusting reflectivity based solely on the VPRs derived using observed refractive conditions yielded the most accurate radar-based estimates of bird density.**

***Index Terms*—Algorithms, animals, correlation, Doppler radar, radar data processing, refractivity.**

I. Introduction

THERE has been renewed interest in the use of radar as a biological research tool [1]–[3] since the current network of weather surveillance radars (WSR-88D, which were designed in 1988 and are Doppler capable) within the U.S. was established due to substantial improvements from its predecessor, including an enhanced capacity to detect clear-air echoes, such as birds and insects [4]. These radars have the capacity to relate the radar reflectivities of birds shortly after the onset of migratory flight to the bird density on the ground before takeoff [5]–[7]. In this way, radar data could provide a spatially explicit assessment of the importance of sites where birds stop over during their migratory journey across a large geographic area, in part, by observing the relative magnitude and temporal variability of bird density during a migration season [8]. This is possible, because, at a continental scale, many birds initiate migratory flights after sunset by departing their daytime stopover sites en masse in an abrupt exodus that is closely synchronized to the position of the sun [8], [9]. To date, such radar applications have been qualitative and/or largely unpublished [5], [7], [11], [12]. Moreover, empirical evidence that the radar reflectivity at the onset of migration is quantitatively related to the density of migrant birds on the ground (which is, hereinafter, referred to as bird density) is lacking. Quantifying bird density using WSR-88D requires the development of methodologies for reducing the influence of radar measurement biases caused by the behavior of migrating birds and the operational characteristics of the radar, as described by Diehl and Larkin [6].

A major source of bias in measures of radar reflectivity for estimating bird ground density is caused by the increasing altitude of the radar beam above the Earth's surface with increasing range from the radar (i.e., the "range" bias of Diehl and Larkin [6]). At the onset of migration, when migrating birds are located close to the ground, reflectivity values steeply decrease with range, becoming zero at the range where the beam completely passes over the migrating bird layer. This precludes direct comparison of the reflectivity measures across ranges. For quantifying surface rainfall, which is an analogous hydrological radar application, researchers have proposed several range adjustment schemes based on the determination of the vertical profile of reflectivity (VPR) [13]–[16]. The VPR is a function that describes the ratio of the vertical variability of reflectivity with respect to a reference. Because the shape, height, and occultation of the radar beam can be estimated, it is possible to determine the magnitude of the sampling bias based on the VPR. Thus, the radar reflectivities measured aloft at different ranges can be adjusted to equivalent measures that allow for direct comparisons across ranges. However, existing VPR-adjustment schemes need to be adapted in order to derive the high-resolution VPRs necessary for quantifying low-altitude bird density at the onset of migration.

Standard atmospheric refraction of the radar beam is usually assumed when estimating beam geometry (i.e., four-thirds effective Earth radius [17]). However, atmospheric refraction is stronger than standard in the presence of temperature inversions, which commonly occur at sunset and deepen into the early evening hours as a result of radiative cooling [18]. Because the determination of the VPR and associated correction-adjustment factors is sensitive to the dimensions and

Manuscript received July 11, 2008; revised November 5, 2008 and December 18, 2008. First published April 10, 2009; current version published July 23, 2009. This work was supported in part by the Southern Company and the National Fish and Wildlife Foundation through the Power of Flight Bird Conservation Fund and by the USGS National Wetland Research Center and the USDA Natural Resources Conservation Service through the Conservation Effects Assessment Project.

J. J. Buler was with The University of Southern Mississippi, Hattiesburg, MS 39406 USA. He is now with the Department of Entomology and Wildlife Ecology, University of Delaware, Newark, DE 19716 USA (e-mail: jbuler@udel.edu).

R. H. Diehl is with The University of Southern Mississippi, Hattiesburg, MS 39406 USA (e-mail: robert.diehl@usm.edu).

Color versions of one or more of the figures in this paper are available online at http://ieeexplore.ieee.org.

Digital Object Identifier 10.1109/TGRS.2009.2014463

propagation path of the radar's beam, it may not be appropriate to assume standard refractive conditions when adjusting for range bias using the radar data collected shortly after sunset. Alternatively, more accurate beam geometry estimates may be obtained using standard radiosonde observations of the refractive conditions of the atmosphere, despite their relatively coarse temporal and vertical resolution [18].

The displacement of birds from their ground source introduces geographical location errors, particularly at small spatial scales. The horizontal distance that birds fly from the time after takeoff until the radar measurement is made determines the magnitude of the displacement. Assuming a constant rate of ascension and flight direction, the magnitude of displacement should increase with increasing radar range, because birds detected at greater ranges are at higher altitudes and therefore have been flying for a longer time than birds at lower altitudes.

Our objectives were the following: 1) to establish that the radar reflectivity at the onset of migration is quantitatively related to the density of migratory birds on the ground during stopover and 2) to determine whether adjustments on range bias, nonstandard beam refraction, and spatial displacement improve the ground–radar bird density relationship. Additionally, we compared the accuracy of algorithm-derived VPRs determined from WSR-88D data with that of vertical target density profiles observed using a vertically oriented portable radar. In Section II, we describe the study area, radar data screening and sampling process, and other data used in this study. We describe the bias-adjustment algorithm in Section III. We present adjustment evaluation methods and results in Section IV. We summarize the conclusions of the algorithm performance in Section V.

II. Study Area and Data

We studied data from two neighboring WSR-88D radars located in Slidell, LA (30.33667°N 89.82556°W, with identifier KLIX), and Mobile, AL (30.67944°N 88.23792°W, with identifier KMOB), which provided radar coverage along the southern coast of the U.S. for portions of the states of Louisiana, Mississippi, Alabama, and Florida (Fig. 1). In general, the area is characterized by flat-to-rolling topography from sea level up to 130 m above sea level. The topography is cut by numerous small rivers, and the land cover is dominated by pine and mixed pine–hardwood forests. More details about the land cover characteristics of the study area are found in [19].

A. Weather Surveillance Radar

We obtained Level-II radar data collected at the KLIX and KMOB radars during the period of peak land bird migration during the autumns of 2002 and 2003 (from September 1 to October 31), and the springs of 2003 and 2004 (from March 15 to May 15) from the National Climatic Data Center archive. WSR-88D radars transmit horizontally polarized electromagnetic radiation at a wavelength of about 10 cm (s-band) and a nominal peak power of 750 kW with a half-power beamwidth (3 dB) of 0.95° [4]. We used two moments of the returned signal in this study: 1) *radar reflectivity*, which is a measure of radar echo strength that is determined by the density and size of the targets in the sampled airspace, and 2) *mean Doppler radial velocity*, which is a measure of the mean target velocity

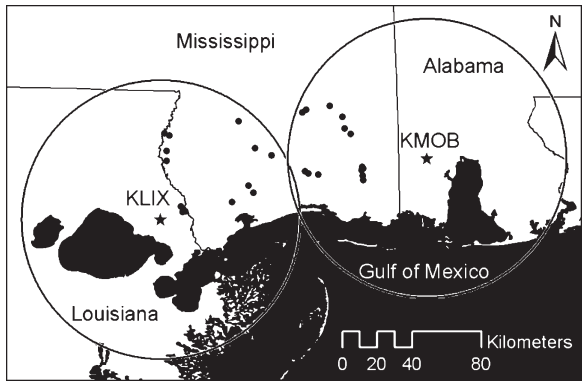

Fig. 1. (Star) Locations and names of two WSR-88D radar stations and their associated 80-km radius coverage areas used in this study. (Dot) Transect sites where we surveyed birds.

relative to the radar. Level-II radar data are collected in polar coordinates with a range resolution of 1 km for reflectivity (0.25 km for velocity) and an azimuth resolution of 0.95°. WSR-88D radars operate in two modes, i.e., "clear air" and "precipitation," providing a "volume scan" comprising a set of 5–14 horizontal 360° sweeps, each of which was collected at different elevation angles ranging from 0.5° up to 19.5°. Volume scans are completed every 6 min (14 sweeps) or 10 min (five sweeps), depending on the radar's mode of operation.

We screened radar data from the 0.5° elevation angle to identify nights when radar reflectivity was dominated by migrating birds and uncontaminated by nonbiological targets (e.g., precipitation, sea breeze fronts, and smoke) and anomalous beam propagation. To distinguish birds from insects, we quantified the target airspeed by vector-subtracting the wind velocity from the target ground velocity. We obtained the wind velocity from radiosonde data (see later). We constructed vertical profiles of the target ground velocity and direction using the methods outlined by Browning and Wexler [20] from vertical azimuth displays (VADs) of the radial velocity data centered on a 1-km-wide focal range window. We used the radial velocity data from the 3.5° elevation angle sweep during the peak of nocturnal migration (∼3 h after sunset) to determine the target ground velocities. This higher elevation angle sweep has less ambiguity in altitude-specific measures of speed and direction and is less affected by refraction and beam occultation than lower elevation angle sweeps. We considered volume scans with mean target airspeeds of more than 6 $\mathrm{m} \cdot \mathrm{s}^{-1}$, as dominated by birds [21], [22].

For all the nights dominated by migrating birds, we carefully selected one volume scan collected within minutes after the apparent onset of nocturnal migration for analysis. There were generally only one or two candidate sweeps from which to choose. Selecting too early, when birds are very close to the ground, would limit the range within which birds could be detected. Selecting too late, when the displacement of the birds from their ground sources is far, would compromise the relationship between radar and ground data. Ultimately, we selected scans between 5 and 15 min after evening civil twilight (i.e., sun elevation between 7° and 9° below the horizon), corresponding as closely as possible to the mean initiation time of nocturnal migration along the Gulf Coast (−8° sun elevation) [10], [23]. Radar data beyond 80 km in range were excluded from the analysis, because the bottom of the radar beam passed above

TABLE I
CLASSIFICATION FREQUENCY (PERCENT) OF SCREENED RADAR DATA TYPES ACROSS NIGHTS BY RADAR STATION AND SEASON. A CAUSE FOR EXCLUDING DATA DUE TO CONTAMINATION WAS SERIALLY DETERMINED BY THE FOLLOWING ORDER OF POTENTIAL SOURCES: PRECIPITATION, ANOMALOUS PROPAGATION, ONGOING BIRD MIGRATION, AND INSECTS. MIXED SOURCES OF CONTAMINATION WERE NOT ELUCIDATED

Data screening classification	Season			
	Autumn		Spring	
	2002	2003	2003	2004
KLIX radar site				
Bird-dominated migration	5 (9%)	6 (11%)	9 (15%)	9 (17%)
No bird migration	1 (2%)	0 (0%)	3 (5%)	4 (7%)
Contaminated data:				
Precipitation	34 (63%)	23 (41%)	18 (30%)	19 (35%)
Anomalous propagation	10 (19%)	17 (30%)	10 (17%)	9 (17%)
Insect-dominated migration	4 (7%)	10 (18%)	7 (11%)	7 (13%)
Ongoing arrival of trans-Gulf migrants	n/a	n/a	13 (22%)	6 (11%)
Total nights screened	54 (100%)	56 (100%)	60 (100%)	54 (100%)
KMOB radar site				
Bird-dominated migration	5 (12%)	7 (15%)	7 (14%)	10 (27%)
No bird migration	1 (2%)	0 (0%)	2 (4%)	1 (3%)
Contaminated data:				
Precipitation	23 (53%)	15 (33%)	18 (35%)	10 (27%)
Anomalous propagation	12 (28%)	13 (28%)	9 (18%)	8 (22%)
Insect-dominated migration	2 (5%)	11 (24%)	7 (14%)	3 (8%)
Ongoing arrival of trans-Gulf migrants	n/a	n/a	8 (16%)	5 (13%)
Total nights screened	43 (100%)	46 (100%)	51 (100%)	37 (100%)

95% of the birds in the airspace at this range under the weakest observed refractive conditions.

Overall, 14% of the screened nights met the selection criteria for analysis (Table I). We rejected most nights due to the presence of precipitation or anomalous propagation of the radar beam. Of the remainder, the absence of migrating birds or the dominant presence of insects occurred 41% of the time. During spring, we rejected additional nights, because, often, there were migrating birds in the air arriving after sunset from trans-Gulf flights that mixed with birds initiating migratory flight.

B. Radiosonde

We obtained radiosonde data at the KLIX radar station from the archive of the University of Wyoming, Laramie. We used radiosonde data to compute the vertical refractive-index gradient of the atmosphere for modeling radar beam propagation and to determine wind speed and direction aloft. Data were sampled at 0000 Coordinated Universal Time (UTC), generally within an hour of the onset of bird migration and within 3 h of radar volume scans used for target identification. We represented the vertical refractive-index gradient as a piecewise linear model of dn/dh. We determined the refractive index of the air n for each radar sample as a function of temperature, pressure, and humidity at each altitude measure (above sea level) h from the corresponding radiosonde data set following that of Bean and Dutton [24].

C. Vertically Oriented Portable Radar

We sampled the vertical distribution of targets near the initiation of bird migration using a portable surveillance radar (Furuno FR-2115-BB Series) with a 12-kW 3-cm (X-band) wavelength and a vertically rotating 20° open-array antenna for one night during spring 2005 and for eight nights during autumn 2005 near Hattiesburg, MS (which is approximately 120 km from the KLIX radar). We turned off the radar's sensitivity control to avoid differences in radar sensitivity with distance. We minimized ground clutter by using a line of trees as a radar fence. We digitally captured radar displays using a VisionRGB-pro1 video capture card sampling at 24 frame/min, approximately matching the rotation rate of the radar antenna. We extracted seven radar sweeps from each night for analysis. These sweeps were separated by 1-min intervals and centered about the time of a concurrent KLIX volume scan at the onset of bird migration. We analyzed concurrent KLIX data to assure that the targets were dominated by birds.

We constructed vertical profiles of the target density by splitting the vertical distribution of targets into 26 height intervals of 50 m that ranged from 100 to 1400 m above ground level (AGL). Accurate sampling of targets below 100 m and above 1400 m was not possible due to ground clutter contamination and the height limitation of the radar display, respectively. Only 2.5% of the targets (200 out of 7786) were detected above 1250 m. We divided the number of radar targets by the volume of the sampled airspace (calculated using the nominal beamwidth provided by the manufacturer) within each height interval to obtain the target density. We then divided the target density at each height interval by the mean target density across all intervals to derive a density ratio profile that is analogous to a VPR. We did not quantify the detection loss of targets with increasing height for the portable radar. However, we found that adjusting the target densities using an approximation of the detection probability function of a similar vertically oriented portable radar from Harmata *et al.* [25] negligibly changed the target density ratio profiles. This is because 91% of our radar targets were detected below 500 m, where detection probability

likely remains near 90%. Therefore, we conducted all the analyses using unadjusted target density ratio profiles.

D. Bird Survey

We obtained migrant bird density data from a concurrent study in which observers conducted bird surveys for two autumn seasons (from early September to the end of October 2002 and 2003) and two spring seasons (from mid-March to early May 2003 and 2004). Field sampling included 24 strip transects measuring 500 m long and 50 m wide within hardwood forests in the study area (see [19] for details). Each radar site had 12 transects within 80 km of the radar that were divided among high-bird-density sites within contiguous bottomland forests and low-bird-density sites within narrow riparian forests along lower order tributaries. Individual transects were surveyed every two to three days. We included only observations of migratory species in the analysis (i.e., we excluded resident species). However, locally breeding/wintering individuals of migratory species could not be distinguished from transient individuals. We calculated the mean migratory bird density adjusted for bird detection probabilities [26] as the number of birds per hectare at each transect across all visits within a season by year for analysis.

We expected that the bird density estimates on the ground were representative of the densities of birds taking off into the radar beam, even though the birds were sampled within a small area (2.5 ha) relative to the area of corresponding radar sampling units (i.e., mean $= 18.5$ ha and range $= 2.2-34.9$ ha), which are referred to as pulse volumes hereinafter. This is because the birds were sampled within a hardwood forest habitat, which comprised the majority $(\text{mean} \pm \text{SD} = 76 \pm 28\%)$ of the land cover beneath the pulse volumes located over transect sites. The relative dominance of the hardwood forest habitat beneath pulse volumes should have minimized errors in bird density estimates due to the contribution of birds in the radar beam that are from other habitat types, where birds may occur at different densities.

III. Algorithm Description

We designed an algorithm for adjusting radar reflectivity measures within individual elevation angle sweeps to equivalent measures with respect to a common height reference across all range distances. The algorithm derives a high-resolution VPR characterizing the change in bird density with altitude and computes individual sampling adjustment factors for every pulse volume. We wrote the algorithm using SAS 9.1. We classified the algorithm into three processing components described here.

A. Spatial Alignment

Before calculating the VPR, the algorithm assembles reflectivity measures into a fixed polar grid with quarter-degree resolution in azimuth and 1-km resolution in range. For example, the reflectivity value of the original 1° pulse volume with a center azimuth of 310.869° is assigned to the four fixed quarter-degree pulse volumes with centers of 310.375°, 310.625°, 310.875°, and 311.125°. This spatial realignment of the original pulse volumes at increased azimuth resolution mitigates the small mechanical variability in horizontal azimuth sampling and allows for easy compilation and analysis of pulse volume data within and among volume scans.

B. Derivation of the VPR

We derived a mean VPR by integrating close-range reflectivity data from the five lowest elevation angle sweeps, similar to Joss and Lee [15]. We determined from preliminary analysis that the data from pulse volumes located over land and between the 5- and 20-km range from the radar produce the most accurate derived VPRs relative to the VPRs observed with the vertically pointed X-band radar (which will be discussed later). We limited the data to the five lowest elevation angles sweeps, because these are the only consistently sampled elevation angles among the different volume scan strategies.

Before integrating data across ranges and sweeps, we averaged the reflectivity values across the pulse volumes at each range by elevation angle sweep. We treated the pulse volumes with missing data as having a reflectivity value of zero. The algorithm trims 25% of the reflectivity values in each tail of the distribution to minimize bias from false zeros due to missing data, as a result of the raw radar data quality control system, and from high reflectivity values (e.g., > 35 dBZ) from unresolved clutter. A large degree of trimming is necessary, because pulse volumes in close proximity to the radar at the lowest elevation angle sweep are particularly susceptible to these biases.

We used two different approaches to model radar beam propagation when estimating the heights of the upper and lower limits of the half-power beamwidth sampled by the radar at each range. The simple approach estimates beam propagation paths, assuming a standard refractive atmosphere where the beam follows a curve with an effective Earth radius of

$$a_e = \frac{4}{3}a \tag{1}$$

where a is the Earth radius. Additionally, the algorithm models beam propagation paths using a piecewise linear model of the refractive-index gradient constructed from radiosonde observations, assuming a spherically stratified atmosphere and spatial homogeneity of the refractive-index gradient within the radar domain following that of Doviak and Zrnic [17], i.e.,

$$s'(h') = \left(\frac{\cos' \theta_e}{1+ra'}\right)\left\{\left[a'^2 \sin^2\theta_e + 2a'(1+ra')h'\right]^{1/2} - a' \sin' \theta_e\right\} \tag{2}$$

where $s'(h')$ is the arc distance from the point of emergence of the beam from the refractive layer below, r is the refractive gradient within the layer, h' is the height above h_b, with h_b being the height AGL of the top of the refractive layer below, $a' = a + h_b$, and θ'_e is the angle made by the beam emerging at height h_b. Angle θ'_e is given by

$$\theta'_e = \tan^{-1}(dh/ds) \tag{3}$$

which can be approximated by the following:

$$\theta'_e \cong \tan^{-1}\left\{\left[a^2 \sin^2 \theta_e + 2ah_b(1 + r_b a)\right]^{1/2}/a \cos\theta_e\right\} \tag{4}$$

where θ_e is the angle from the refractive layer below, and r_b is the refractive gradient in the layer below.

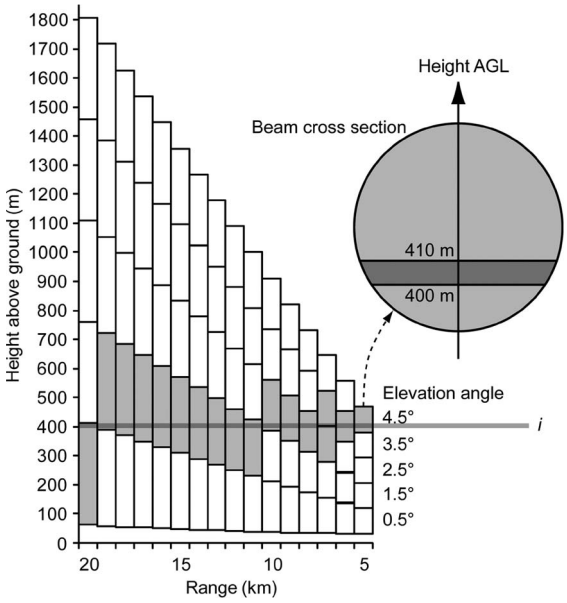

Fig. 2. Example principle of calculation of VPR. Pulse volumes within D_i, where $i = 41$, are shaded in gray. The radar beam cross section depicts β, i.e., the proportion of the beam within height interval i, for the pulse volume at 4.5° elevation and 5-km range.

After compiling mean reflectivity $\overline{Z}_c$ and the beam height for each range distance and elevation angle combination c, the algorithm derives the mean VPR represented by the following discrete function:

$$z(i) = \frac{\bar{Z}_i(D_i) n_z}{\sum_{i=1}^{n_z} \bar{Z}_i(D_i)} \tag{5}$$

where i denotes the height AGL interval $[h_i^-, h_i^+]$ such that $h_i^- = (i-1)\Delta h$ and $h_i^+ = h_i^- + \Delta h$, with Δh being the increment of the height discretization; n_z is the number of height intervals; and $\overline{Z}_i(D_i)$ is the beam-area-weighted mean reflectivity of domain D_i grouping all of the pulse volumes among the five elevation angle sweeps that measure reflectivity within height interval i (Fig. 2), which is given by

$$\bar{Z}_i(D_i) = \frac{\sum_{c=1}^{n_c} \bar{Z}_c \beta_{ci}}{\sum_{c=1}^{n_c} \beta_{ci}} \tag{6}$$

where β_{ci} is the proportion of the beam cross section within height interval i for a given range and elevation angle combination c (see [14, pp. 237–238] for details on the computation of β), and n_c is the number of range and elevation angle combinations. It is assumed that the VPR is the same at any point within the radar domain and independent of the horizontal variability of reflectivity. The algorithm derives the VPRs at height increments Δh of 10 m within the height range of 0–1750 m AGL (the approximate height of the upper limit of a 0.95° beam inclined 0.48° in elevation within an 80-km range from the radar under standard refractive conditions). We chose a 10-m height interval to enable us to compute different adjustment factors for pulse volumes from adjacent ranges, because the minimum difference in the total beam height between any two adjacent ranges is 18 m. Reflectivity is assumed to be constant below the minimum height sampled (which is usually less than 50 m AGL). The algorithm derives an initial mean VPR, assuming uniform target density and power distribution in the beam. However, because the actual target density is not uniform within the beam, the reflectivity data are reintegrated by the weighting target density within the beam based on the initial mean VPR.

C. Adjustment on Range Bias

We used the derived mean VPR for each sample to determine the adjustment factors for every combination of range, mean ground height, and amount of beam occultation among pulse volumes at the lowest elevation angle sweep. First, we identified the unique combinations of pulse volume characteristics. The mean ground height for every pulse volume is the elevation above sea level averaged over the Earth surface beneath the pulse volume and is determined to the nearest 10 m using the elevation data from the National Elevation Data set (1-sec^{-1} resolution) assembled by the USGS. The percent area of the radar beam cross section occluded by topography is a function of the radius of the beam and the difference of the average height of the ground within a given pulse volume and the center of the radar beam. We calculated beam occultation to the nearest 0.1% using the simplified beam interception function outlined by Bech *et al.* [27] under standard and observed atmospheric conditions. Although the estimated maximum beam occultation under the most severe refractive conditions was negligible (4.0%), we retained this step, because beam occultation is more substantial at other radar sites. Finally, we eliminated unresolved clutter such as echoes from the raw data at the lowest elevation angle sweep if the reflectivity value of a given pulse volume was seven times greater than that of half of the immediately surrounding pulse volumes. This threshold is conservative enough to remove most of the clutter, e.g., the clutter caused by vehicles on road overpasses, while retaining most of the biological echoes.

The adjustment factor is the beam-area-weighted mean VPR ratio sampled by the beam for a given pulse volume and can be expressed by the following function:

$$z(d, g, o) = \sum_{i=1}^{n_z} z_i \beta_i \tag{7}$$

where d is the range, g is the mean ground height, o is the amount of beam occultation, z_i is the VPR ratio at height interval i, and β_i is the proportion of the beam cross section at i. By dividing the raw reflectivity of each pulse volume by its adjustment factor, the algorithm estimates the reflectivity of birds in the airspace from 0 to 1750 m AGL.

IV. Evaluation of Algorithm Performance

A. Validation of Derived VPRs

To determine the optimal data range for deriving profiles, we derived VPR curves from WSR-88D data under the observed refractive conditions for a series of range combinations $(n = 210)$ and compared them to concurrent target density profiles observed with a vertically scanning portable radar. We evaluated the goodness of fit between the derived VPRs and the

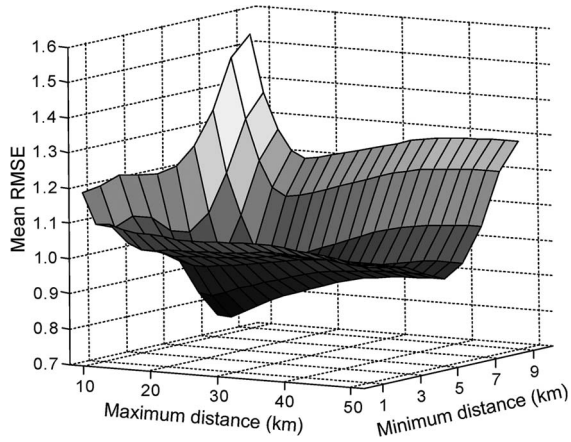

Fig. 3. Response surface of the mean RMSE between VPRs observed with a vertically pointed portable radar ($n = 9$) and VPRs derived using KLIX radar data from the five lowest elevation angle sweeps for all range combinations between a given minimum and maximum distance from the KLIX radar.

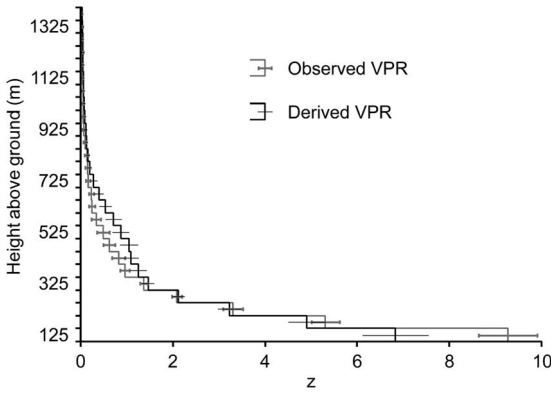

Fig. 4. Mean (± 1 standard error) observed and derived VPRs of birds near the onset of migration. The derived mean VPRs were determined using reflectivity data from the five lowest elevation angle sweeps between 5 and 20 km from the radar and modeling beam propagation using the observed refractive conditions. The VPRs were observed during nine nights in 2005 at Hattiesburg, MS.

observed target density profiles using the root-mean-square error (RMSE). Minimum distances ranged from 1 to 10 km from the weather radar at 1-km intervals. Maximum distances ranged from 10 to 50 km from the weather radar at 2-km intervals. For this analysis, we derived VPRs at height increments of 50 m, with a reference height range of 100–1400 m AGL to match the resolution and profile range of the observed target density profiles obtained from the portable radar. The mean RMSE across the nine sampling nights for all data range combinations ranged from 0.79 to 1.53. The response surface of the mean RMSE exhibits a well-defined valley (i.e., best fit) near the subset data range of 5–20 km (Fig. 3). Thus, we used this subset data range for deriving VPRs for subsequent analyses.

The VPR derived by integrating data between 5 and 20 km from the radar matched the mean observed target density profile well, despite the 120-km distance between the location of the portable marine radar observations and the location of the KLIX radar station (Fig. 4). Thus, the VPR appears to be relatively homogeneous over space. Upon closer examination, the derived VPRs at KLIX slightly overestimated the observed profile ratios at around 500 m AGL, which we attribute to consistent and subtle spatial heterogeneity in the structure of the reflectivity field. This spatial heterogeneity of reflectivity

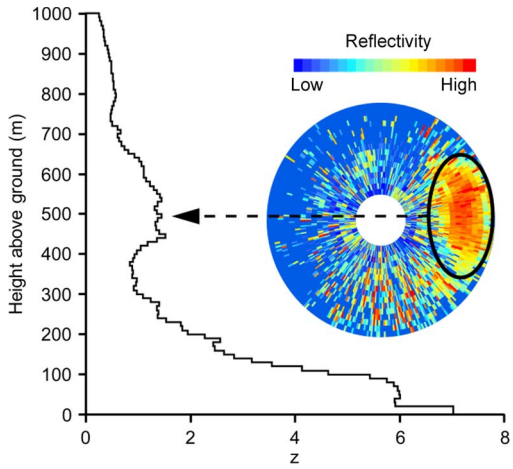

Fig. 5. Example of the effect of spatial heterogeneity in reflectivity on the derivation of the VPR. (Right) The plan position indicator display shows radar reflectivity from the 3.5° elevation angle sweep between 5 and 20 km from the KMOB radar taken at 01:03:33 UTC on 1 April 2003. The area of high reflectivity in the east (circled region) is over a large patch of forested wetland habitat and exerts its influence when integrating volume scan data by the presence of (left) a peak in the derived VPR averaged across all azimuths between 400 and 600 m AGL.

is due to the differential distribution of birds within stopover habitats around the radar. We observed occasional instances of marked spatial heterogeneity, most often during spring at KMOB, which were characterized by areas of relatively high reflectivity in association with distinct areas known to harbor high migratory bird densities (e.g., a forested wetland habitat or areas in close proximity to coastal waters [19]). Fig. 5 shows an extreme example where there is a large area of high reflectivity to the east of the radar over a forested wetland habitat. The influence of this spatial heterogeneity is translated into the presence of a second general peak in the derived VPR ratios between 400 and 600 m AGL.

B. Differences in Beam Propagation Models

We observed superrefractive gradients on 87% of the sampling nights, which caused the average modeled height of the lower limit of the radar beam to be significantly lower than the standard beam height [Fig. 6(a)]. The absolute magnitude of this height difference increased with increasing range. While the difference in beam propagation yielded slight differences in the derived VPRs between models, it produced significant range-dependent differences in the magnitude of adjustment factors [Fig. 6(b)]. In general, adjustment factors based on the observed refractive conditions increased with range, which resulted in lower adjusted reflectivity with increasing range relative to that based on standard refraction.

C. Range Dependence of Radar Data

Unadjusted radar reflectivity declined with increasing distance from the radar [Fig. 7(a)] with a mean ($\pm$SE) correlation of -0.46 ± 0.05 between unadjusted reflectivity and radar range. Adjusting the reflectivity data using the derived VPRs was effective in removing this range dependence [Fig. 7(b)]. The mean correlation between the VPR-adjusted data and the radar range was not significantly different from zero under standard refractive conditions (mean $= 0.01 \pm 0.07$, $t = 0.15$,

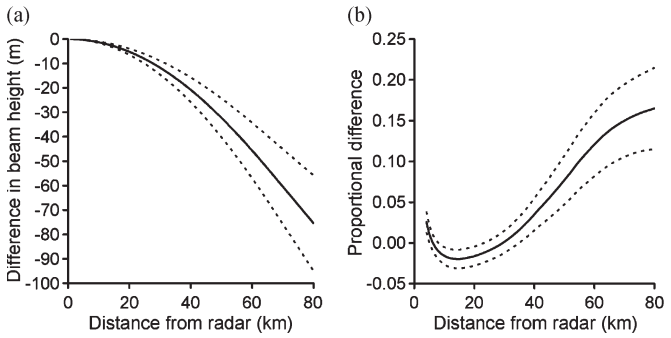

Fig. 6. (a) Mean difference in the estimated height of the lower limit of the radar beam between the observed refraction model and the standard refraction model across 29 sampling nights. (b) Mean proportional difference in reflectivity adjustment factors between the observed refraction model and the standard refraction model across 29 sampling nights $[z_{\mathrm{observed}} - z_{\mathrm{standard}}]/z_{\mathrm{standard}}$. The dotted lines in both plots denote one standard error above and below the mean.

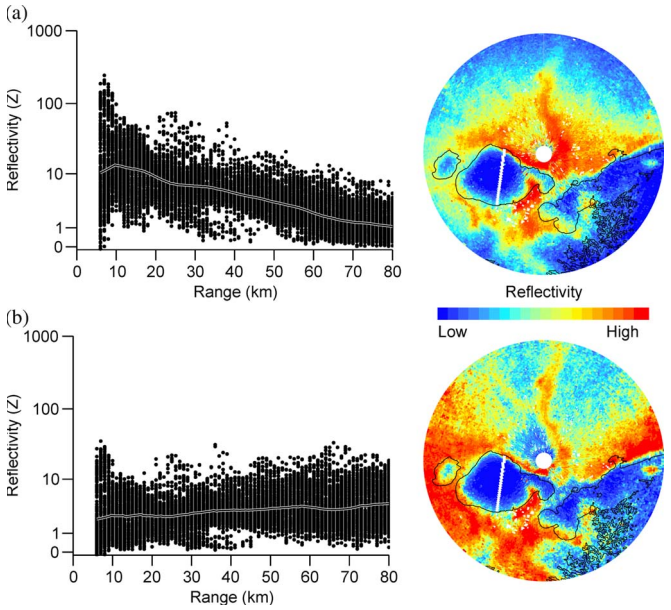

Fig. 7. (a) Unadjusted radar reflectivity averaged across 18 nights during the springs of 2002 and 2003 at KLIX declines with range from the radar. (b) Same radar reflectivity data adjusted for the VPR using the observed refractive conditions does not decline with range from the radar. Only 15% of all data are shown in scatterplots. (Fit line) Moving averages. (White area) Static clutter within the plan position indicator displays of radar data at an elevation angle of 0.5°. (Black line) Coastline.

and $P = 0.889$) or observed refractive conditions (mean $= -0.08 \pm 0.08$, $t = -0.95$, and $P = 0.372$).

D. Evaluation of the Relationship Between Radar Reflectivity and Bird Density

1) Approach: We analyzed the correspondence between radar and ground data across survey sites within seasons (i.e., space) rather than across days within survey sites (i.e., time) because of the potential disparity between bird density and migratory activity on a given day, particularly in relation to weather [28]. For example, in adverse weather, large numbers of resting migratory birds can be counted on the ground. However, weak reflectivities will be measured by radars, because few birds will initiate migration. On the other hand, strong reflectivities can be detected with radars when the ground numbers are only moderate, but the weather conditions are optimal for takeoff. Using seasonal averages of bird densities and radar reflectivities should thus provide a better correlation between the number of resting birds on the ground and the radar-based density of departing migrants.

We computed the seasonal mean radar reflectivity associated with each transect site by converting vector-based pulse volume radar data into raster grids with 30-m cell resolution and averaging the nonclutter reflectivity values of cells located within transect boundaries using ArcMap 9.2. We filtered radar data for static clutter and beam blockage beyond the dynamic clutter filtering performed during previous data processing. We did this by analyzing the probability of detecting reflectivity (POD) and the mean reflectivity value across approximately 4000 daytime volume scans collected during June 2003 and 2004 (i.e., when birds were not migrating through the study area) for each pulse volume. There were two classes of static clutter: 1) pulse volumes with a high POD and a mean detected reflectivity greater than 30 dBZ (associated with persistent returns from ground targets) and 2) pulse volumes with an extremely low POD (associated with frequent rejection of data as part of the automated real time clutter rejection system or with areas where the radar beam is substantially blocked). Reflectivity data from pulse volumes containing static clutter or beam blockage were excluded from regression analyses. The POD analysis revealed that two survey transects within the KMOB radar domain fell within regions of noticeable beam blockage that could not be accounted for by topography. Data from these transects were not included in regression analyses. This left KMOB with ten transect sites for analysis for a given sampling season among 11 unique transect sites overall.

The ground survey data set was originally designed for a different study, so we tested for correlation between range and bird density prior to assessing adjustments to reflectivity data. Unfortunately, bird density was negatively correlated with radar range for all seasons at KLIX (Pearson r ranged from -0.70 to -0.91) and positively correlated with radar range for the two autumn seasons at KMOB (Pearson $r = 0.54$ and 0.73). These correlations of the ground data with range would confound goodness-of-fit estimates between ground and radar data because of the negative range dependence inherent in the unadjusted radar data. Therefore, we statistically controlled the range dependence of the ground data set by drawing random samples of ten cases with replacement from the original transect survey data to generate 2000 bootstrap samples in which there was no significant correlation ($P > 0.1$) between bird density and distance from the radar. We then averaged regression model parameters across the collection of bootstrap samples for each radar site, season, and year combination (i.e., the sampling season; $n = 8$).

We modeled the relationship between the seasonal mean radar reflectivity observed at the onset of nocturnal bird migration (dependent variable) and the seasonal mean migratory bird density measured from ground transect surveys (independent variable) using linear regression through the origin because of the following conditions: 1) Reflectivity represents a direct proportion of the density of birds aloft [2], [29]. 2) We fit individual simple linear regressions for each replicate sampling season and nearly always found that y-intercepts were not

significantly different from zero. For each replicate sampling season, we fit regression models between ground bird density and radar reflectivity using unadjusted radar data and radar data adjusted for the vertical reflectivity profile under the following four different schemes:

1) profile adjustment using standard refractive conditions;
2) profile adjustment using standard refractive conditions with a spatial adjustment of the displacement of birds;
3) profile adjustment using observed refractive conditions;
4) profile adjustment using observed refractive conditions with a spatial adjustment of the displacement of birds.

To account for the displacement of birds from their areas of departure on the ground, we moved the spatial locations of individual pulse volumes for each volume scan in the reverse direction and distance that we estimated the birds to have traversed after departing their habitats. We estimated the median flight time by dividing the VPR-determined median height of the birds sampled within each pulse volume by 1 m/s, which is the mean vertical ascent rate of a typical land bird at the onset of migration [30]–[32]. We determined the VPR-weighted mean ground speed and direction of the target movement from the VAD of the 3.5° elevation angle sweep at the onset of migration. We multiplied the mean target ground speed by the median flight time of the birds sampled within each pulse volume to estimate individual adjustment distances. We filled the data gaps between spatially adjusted polygons after grid conversion using the median value of nonmissing reflectivities within a 10×10 cell window around the target cells.

We tested for correlation between the coefficients of variation (CVs) of radar reflectivity and bird density to evaluate how well radar observations capture the variability of bird density within a season. We pooled radar and survey observations across years by radar site and migration season (e.g., autumn and spring), because the sample sizes were low during a given season. Moreover, because the CV of bird density was not range dependent, we did not perform bootstrap sampling.

2) Results: Among sampling seasons and radars, there were significant positive linear relationships between seasonal mean radar reflectivity and ground bird density for both unadjusted radar data (bootstrap mean R^2 ranged from 0.635 to 0.911) and adjusted radar data (bootstrap mean R^2 ranged from 0.701 to 0.966). However, the regression coefficients of the relationship between reflectivity and bird density considerably varied among individual sampling seasons. The magnitude of the coefficient for the profile adjustment using the observed refractive conditions varied by a factor of 18 from 1.16 to 20.94 among sampling seasons. For a given season, the coefficients from KMOB data were greater than those from KLIX by a mean of 3.3. The coefficients during autumn were greater (mean $= 9.83$) and more variable (CV $= 0.80$) than the coefficients during spring (mean $= 2.43$ and CV $= 0.48$).

The significance of correlations between the CV of radar reflectivity and that of bird density were mixed but trended positive. Specifically, the correlations from KMOB were marginally significant (autumn: Pearson $r = 0.58$, $n = 12$, and $P = 0.048$; spring: $r = 0.55$, $n = 12$, and $P = 0.062$), whereas those from KLIX were not significant (autumn: $r = 0.41$, $n = 11$, and $P = 0.214$; spring: $r = 0.54$, $n = 11$, and $P = 0.086$). The within-season variability of bird density at ground survey sites was greater during autumn compared with spring (mean paired difference in CV $= 14.0 \pm 4.4\%$, $t = 3.18$, $df = 22$, and $P = 0.004$). However, the within-season variability between autumn and spring for radar reflectivity associated at survey sites was not significantly different, although it followed the same trend (mean paired difference in CV $= 8.3 \pm 7.9\%$, $t = 1.05$, $df = 22$, and $P = 0.305$).

E. Goodness of Fit Between Radar Estimates and Ground Observations

We evaluated the goodness of fit between radar-based bird density estimates and ground survey bird density measures using RMSE. We derived bird density estimates based on radar reflectivity by inverting fitted regression models. For each season, we assessed the bootstrap-mean RMSE of radar estimates based on unadjusted radar data and adjusted radar data under the four different vertical reflectivity profile schemes.

All four profile adjustments significantly improved the accuracy of bird density estimates compared with estimates based on unadjusted radar data (Table II). The greatest and most consistent overall improvement was achieved by adjusting radar data with profiles using near-real-time observed refractive conditions only; the mean (±SE) RMSE improved by $33 \pm 4\%$ over unadjusted data ($t = 8.51$, $df = 7$, and $P < 0.001$). The simplest adjustment of radar data using the profile derived, assuming standard refractive conditions, exhibited similar improvement, i.e., $31 \pm 5\%$ ($t = 5.58$, $df = 7$, and $P < 0.001$). The adjustment schemes with spatial adjustment of data to account for the displacement of birds exhibited the least and most variable improvements. However, a more-detailed site-specific analysis reveals that the pattern of relative improvement in accuracy of bird density estimates among the adjustment schemes contrasted. At KLIX, the bird density estimates based on the adjustment using the observed refractive conditions with a spatial adjustment of the displacement of birds had the strongest relationship to the observed bird densities of the four adjustment schemes (Fig. 8). However, at KMOB, this adjustment scheme exhibited the weakest relationship (Fig. 9). Instead, the bird density estimates based on the simplest adjustment using standard refraction had the strongest relationship to the observed bird densities at KMOB, whereas this adjustment scheme exhibited the weakest relationship at KLIX.

Because superrefractive conditions were common across sampling nights, it is not surprising that the most accurate overall data adjustment was based on near-real-time observations of refractive conditions. This was the case at KLIX, where atmospheric soundings were made at the radar site within an hour of volume scans. At KMOB, however, the "observed" refractive conditions used when adjusting radar data were from the KLIX radar located approximately 150 km away. Given that the representativeness of sounding data declines with distance from the sounding site [33], the "observed" refractive conditions may have been less representative of the actual refractive conditions than assuming standard refraction at KMOB. This may explain the greater accuracy of data adjusted using standard refraction at KMOB.

We expected that adjusting data for spatial displacement would improve the ground–radar bird density relationship, because birds are differentially displaced from their point of departure on the ground according to their ground speed, flight

TABLE II
MEAN RMSE OF RADAR-BASED BIRD DENSITY ESTIMATES FOR UNADJUSTED AND FOUR VPR ADJUSTMENT SCHEMES BASED ON 2000 BOOTSTRAPPED SAMPLES BY RADAR, SEASON, AND YEAR. THE PERCENT REDUCTION IN RMSE FROM THE UNADJUSTED SCHEME IS PRESENTED IN PARENTHESES, WITH ONE-TAILED PROBABILITY VALUES P OF PAIRED T-TESTS INDICATED FOR AVERAGED DATA

Radar	Season	Year	No adjustment (raw data)	Vertical-profile adjustment			
				Using standard refraction		Using observed refraction	
				Without spatial displacement	With spatial displacement	Without spatial displacement	With spatial displacement
KLIX	Autumn	2002	0.758	0.425 (44%)	0.497 (34%)	0.397 (48%)	0.531 (30%)
	Autumn	2003	0.853	0.571 (33%)	0.423 (50%)	0.568 (33%)	0.413 (52%)
	Spring	2003	0.686	0.755 (-10%)	0.704 (-3%)	0.617 (10%)	0.568 (17%)
	Spring	2004	0.522	0.275 (47%)	0.227 (57%)	0.278 (47%)	0.229 (56%)
	Average		**0.705**	**0.507 (28%)**	**0.463 (34%)***	**0.465 (34%)****	**0.435 (38%)****
KMOB	Autumn	2002	0.690	0.470 (32%)	0.551 (20%)	0.492 (29%)	0.574 (17%)
	Autumn	2003	0.728	0.424 (42%)	0.343 (53%)	0.454 (38%)	0.421 (42%)
	Spring	2003	0.406	0.321 (21%)	0.594 (-46%)	0.321 (21%)	0.596 (-47%)
	Spring	2004	0.338	0.200 (41%)	0.302 (11%)	0.201 (40%)	0.312 (8%)
	Average		**0.540**	**0.354 (34%)****	**0.447 (17%)**	**0.367 (32%)****	**0.476 (12%)**
Total average			**0.622**	**0.430 (31%)****	**0.455 (27%)***	**0.416 (33%)****	**0.456 (27%)****

* $P \leq 0.05$
** $P < 0.025$

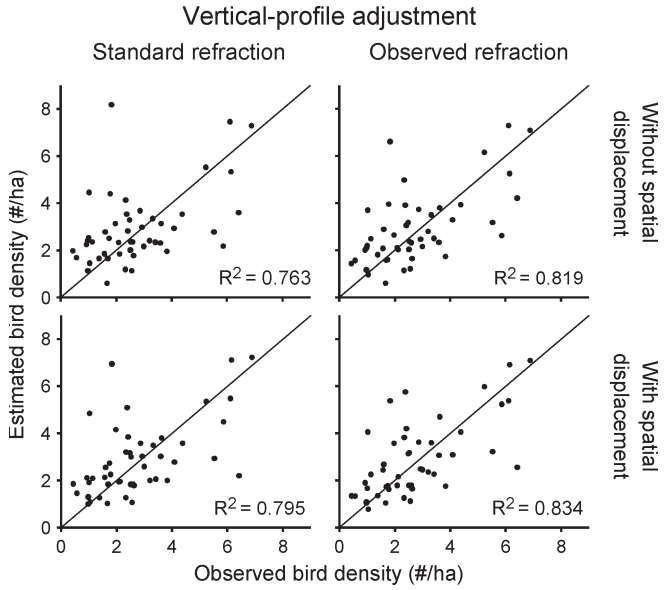

Fig. 8. Scatterplots of radar-estimated versus observed seasonal-mean bird density for radar data adjusted under four different schemes: adjusted for VPR using standard or observed refraction and with or without an additional spatial adjustment of the displacement of birds. Data are from KLIX and pooled across seasons.

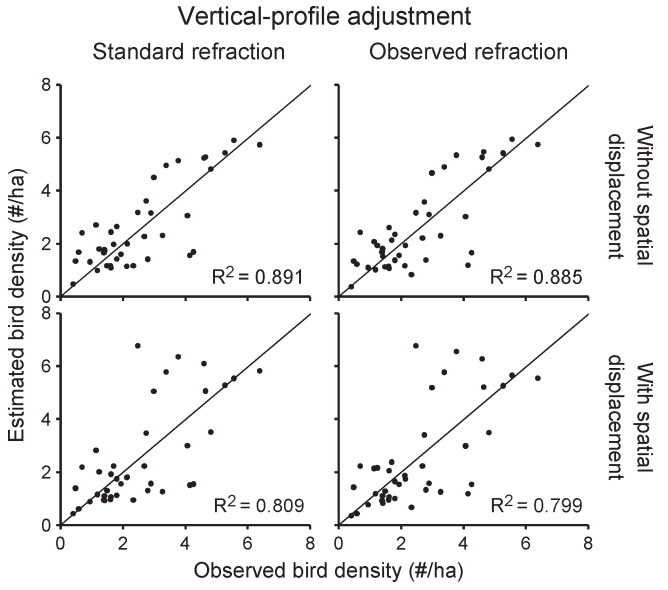

Fig. 9. Scatterplots of radar-estimated versus observed seasonal-mean bird density for radar data adjusted under four different schemes: adjusted for VPR using standard or observed refraction and with or without an additional spatial adjustment for displacement of birds. Data are from KMOB and pooled across seasons.

direction, and time aloft (i.e., flight altitude). This was the case at KLIX for three out of four sampling seasons but for only one out of four sampling seasons at KMOB. We attribute this contrasting performance of the spatial displacement adjustment to radar site differences in how well the derived VPRs represented the actual vertical distributions of targets. The spatial displacement adjustment is particularly sensitive to the accuracy of the derived VPR. Therefore, a high degree of spatial heterogeneity of reflectivity, which reduces the accuracy of the derived VPR, could lead to spurious displacement adjustments. This may explain why the spatial displacement adjustments poorly performed at KMOB, where reflectivity was more spatially heterogeneous than at KLIX.

V. CONCLUSION

The radar reflectivity measured at the onset of nocturnal land bird migration was positively related to the density of migratory birds on the ground. This finding provides empirical support for using radar data to map where birds stop over during

their migratory journeys in order to identify important sites for conservation and better understand their stopover habitat use. This is just one of the many applications of weather surveillance radar data that are of increasing interest to biologists investigating the ecology and behavior of birds, insects, and bats in the aerosphere.

However, weather surveillance radars quantify echoes caused by layered biological targets such as migrating birds in a manner that introduces bias in radar measures. We evaluated four combinations of an algorithm to improve the relationship between reflectivity and ground bird density by adjusting radar measures for range bias using VPRs based on standard or observed beam refraction, with or without accounting for the spatial displacement of birds from their ground source. All four of the bias-adjustment schemes produced significant improvement in the accuracy of bird density estimates relative to unadjusted radar data. These improvements were likely underestimated due to confounding correlations of ground bird density data with distance from the radar, which we attempted to statistically control. In general, adjusting reflectivity based on VPRs derived using observed refractive conditions yielded the most accurate radar-based estimates of bird density. However, adjusting reflectivities using standard refraction achieved 90% of the improvement obtained using observed refractive conditions, even though superrefractive conditions were frequently present. Although it appears that effective radar data adjustments are possible by assuming standard refraction, evaluation of these adjustments would benefit from further analyses that include more ground validation sites at longer ranges from the radar (i.e., where the largest differences in beam propagation models occur). Moreover, we acknowledge the need for better ground data sampling that intentionally avoids any confounding range dependence with bird density. Using standard refraction allows for adjusting reflectivity data from radars where radiosonde observations are absent and provides more accurate estimates than trying to apply the observed refraction conditions from a distant location. Our methods for adjusting reflectivity measures could be used for other biological applications in which spatially explicit quantitative density estimates of flying animals exhibiting well-synchronized movements are desired (e.g., waterfowl feeding flights and insect migration).

Spatial heterogeneity of reflectivity data near the radar reduces the representativeness of the derived VPRs. This led to decreased performance of the spatial adjustment of the displacement of birds from their ground source. Spatial displacement adjustment schemes had the weakest performance when reflectivity was noticeably heterogeneous. Conversely, when reflectivity was relatively homogeneous and the representativeness of the derived VPRs was presumably high, the adjustment schemes with spatial displacement outperformed the counterpart schemes without spatial displacement. The influence of spatial heterogeneity in reflectivity data on the derivation of VPRs may be reduced using a ratio of reflectivity at two or more elevation angles to indirectly identify the most probable VPR [13], [14].

Regression coefficient values between reflectivity and bird density widely varied among sampling seasons and radars. Therefore, we urge caution in directly comparing reflectivity measures between radars, seasons, or even individual days in the absence of ground data calibration when evaluating relative bird densities during migratory exodus. However, direct comparisons of relative differences in reflectivity measures within individual radar samples in the absence of ground data calibration can be made. We attribute the variability in the reflectivity–bird density relationship to sampling error or bias from small sample sizes, spatial variation in the timing of the initiation of migratory flight (i.e., "sunset" bias of Diehl and Larkin [6]), and the coarse sampling rate of WSR-88D. For instance, we had proportionally larger sample sizes during spring seasons that generally exhibit greater daily consistency in the magnitude of migratory flights compared with autumn seasons [34]. Consequently, we found lower variability in the reflectivity–bird density relationship among spring seasons compared with autumn seasons. Additionally, the low sampling rate of radar data (mean $= 14\%$ of all nights) relative to ground survey data ($\sim$33–50% of days) for all seasons likely explains the poor correlation between the CV of radar reflectivity and that of bird density.

Because the onset of migration is closely tied to the elevation of the sun [9], [10], [23], spatial variation in sun elevation can introduce bias in reflectivity measures between radars, which accounts for some of the variability that we observed in the reflectivity–bird density relationship. We estimate that, within seasons, the volume scans at KMOB were taken a mean of 5.25 min later than those at KLIX relative to the same time point during the takeoff phase of migration. This assumes that the initiation of migration varied only with respect to the local elevation of the sun, which moves across the Earth's surface at 24 km/min within our study area. Because the number of birds in the airspace doubles every $\sim$2.5 min during the typical 30-min duration of the takeoff phase [9], [10], the relative timing difference should have produced a 3.7-fold increase in the mean regression coefficient value between reflectivity and bird density for KMOB data compared with those for KLIX data. Accordingly, the observed regression coefficients from KMOB data were consistently 3.3 times greater than those from KLIX.

It is also important to recognize that sampling error from timing differences during takeoff could also occur due to the coarse sampling rate of WSR-88D. At a rate of one volume scan every 10 min in clear-air mode, WSR-88D poorly samples the rapid change in the number of birds entering the airspace during takeoff. Moreover, the WSR-88D data collection is not synchronized with the onset of migration. Thus, despite any effort to account for sun elevation to select volume scans nearest to the same relative point during the takeoff phase, there could still be a sampling error of up to 5 min. This may result in a nearly fourfold error in the magnitude of reflectivities. We are currently investigating data interpolation techniques to estimate reflectivity at the same relative time point during the takeoff phase between radar volume scans for individual pulse volumes. This approach should diminish both the sampling error due to the coarse sampling rate of WSR-88D and the bias from geographic differences in the timing of the initiation of migratory flight. It should also allow for direct comparisons of reflectivity measures without ground data calibration.

ACKNOWLEDGMENT

The authors would like to thank three anonymous reviewers for helping improve this paper. The ground survey data were

obtained in collaboration with F. Moore at the University of Southern Mississippi through funding from the NOAA Coastal Impact Assistance Program administered by the Mississippi Department of Environmental Quality.

REFERENCES

[1] S. A. Gauthreaux, J. W. Livingston, and C. G. Belser, "Detection and discrimination of fauna in the aerosphere using Doppler weather surveillance radar," *Integrative Comparative Biol.*, vol. 48, no. 1, pp. 12–23, 2008.

[2] R. H. Diehl, R. P. Larkin, and J. E. Black, "Radar observations of bird migration over the Great Lakes," *Auk*, vol. 120, no. 2, pp. 278–290, 2003.

[3] K. R. Russell, D. S. Mizrahi, and S. A. J. Gauthreaux, "Large-scale mapping of purple martin pre-migratory roosts using WSR-88D weather surveillance radar," *J. Field Ornithol.*, vol. 69, no. 2, pp. 316–325, 1998.

[4] T. D. Crum and R. L. Alberty, "The WSR-88D and the WSR-88D operational support facility," *Bull. Amer. Meteorol. Soc.*, vol. 74, no. 9, pp. 1669–1687, Sep. 1993.

[5] D. N. Bonter, S. A. Gauthreaux, and T. M. Donovan, "Characteristics of important stopover locations for migrating birds: Remote sensing with radar in the Great Lakes basin," *Conservation Biol.*, to be published.

[6] R. H. Diehl and R. P. Larkin"Introduction to the WSR-88D (NEXRAD) for ornithological research," in *Proc. 3rd Int. Partners Flight Conf. March 20-24—Bird Conservation Implementation and Integration in the Americas*, C. J. Ralph and T. D. Rich, Eds. Albany, CA: Pacific Southwest Res. Station, Forest Service, U.S.D.A., 2005, vol. 2, pp. 876–888. Gen. Tech. Rep. PSW-191, Asilomar, California.

[7] S. A. Gauthreaux and C. G. Belser, "Radar ornithology and biological conservation," *Auk*, vol. 120, no. 2, pp. 266–277, 2003.

[8] D. W. Mehlman, S. E. Mabey, D. N. Ewert, C. Duncan, B. Abel, D. Cimprich, R. D. Sutter, and M. S. Woodrey, "Conserving stopover sites for forest-dwelling migratory landbirds," *Auk*, vol. 122, no. 4, pp. 1281–1290, 2005.

[9] S. Åkesson, T. Alerstam, and A. Hedenström, "Flight initiation of nocturnal passerine migrants in relation to celestial orientation conditions at twilight," *J. Avian Biol.*, vol. 27, no. 2, pp. 95–102, 1996.

[10] J. J. Hebrard, "The nightly initiation of passerine migration in spring: A direct visual study," *Ibis*, vol. 113, pp. 8–18, 1971.

[11] R. H. Diehl, "Landscape associations of birds during migratory stopover," Ph.D. dissertation, Univ. Illinois, Urbana, IL, 2003.

[12] J. J. Buler, "Understanding habitat use by landbirds during migration along the Mississippi Gulf Coast using a scale-dependent approach," Ph.D. dissertation, Univ. Southern Mississippi, Hattiesburg, MS, 2006.

[13] B. Vignal, H. Andrieu, and J. D. Creutin, "Identification of vertical profiles of reflectivity from volume scan radar data," *J. Appl. Meteorol.*, vol. 38, no. 8, pp. 1214–1228, Aug. 1999.

[14] H. Andrieu and J. D. Creutin, "Identification of vertical profiles of radar reflectivity for hydrological applications using an inverse method—Part I: Formulation," *J. Appl. Meteorol.*, vol. 34, no. 1, pp. 225–239, Jan. 1995.

[15] J. Joss and R. Lee, "The application of radar-gauge comparisons to operational precipitation profile corrections," *J. Appl. Meteorol.*, vol. 34, no. 12, pp. 2612–2630, 1995.

[16] J. Koistinen, "Operational correction of radar rainfall errors due to vertical reflectivity profile," in *Proc. 25th Int. Conf. Radar Meteorol.*, 1991, pp. 91–94.

[17] R. J. Doviak and D. S. Zrnic, *Doppler Radar and Weather Observations*. San Diego, CA: Academic, 1993.

[18] J. Bech, B. Codina, J. Lorente, and D. Bebbington, "Monthly and daily variations of radar anomalous propagation conditions: How 'normal' is normal propagation?" in *Proc. 2nd Eur. Meteorol. Radar Conf.*, 2002, pp. 35–39.

[19] J. J. Buler, F. R. Moore, and S. Woltmann, "A multi-scale examination of stopover habitat use by birds," *Ecology*, vol. 88, no. 7, pp. 1789–1802, Jul. 2007.

[20] K. A. Browning and R. Wexler, "The determination of kinematic properties of a wind field using Doppler radar," *J. Appl. Meteorol.*, vol. 7, no. 1, pp. 105–113, Feb. 1968.

[21] R. P. Larkin, "Flight speeds observed with radar, a correction: Slow 'birds' are insects," *Behav. Ecol. Sociobiol.*, vol. 29, no. 3, pp. 221–224, Oct. 1991.

[22] S. A. Gauthreaux and C. G. Belser, "Displays of bird movements on the WSR-88D: Patterns and quantification," *Weather Forecast.*, vol. 13, no. 2, pp. 453–464, Jun. 1998.

[23] S. A. J. Gauthreaux, "A radar and direct visual study of passerine spring migration in Southern Louisiana," *Auk*, vol. 88, pp. 343–365, 1971.

[24] B. R. Bean and E. J. Dutton, *Radio Meteorology*. Washington, DC: U.S. Govt. Printing Office, 1966.

[25] A. R. Harmata, K. M. Podruzny, J. R. Zelenak, and M. L. Morrison, "Using marine surveillance radar to study bird movements and impact assessment," *Wildlife Soc. Bull.*, vol. 27, pp. 44–52, 1999.

[26] S. T. Buckland, D. R. Anderson, K. P. Burnham, J. L. Laake, D. L. Borchers, and L. Thomas, *Introduction to Distance Sampling*. New York: Oxford Univ. Press, 2001.

[27] J. Bech, B. Codina, J. Lorente, and D. Bebbington, "The sensitivity of single polarization weather radar beam blockage correction to variability in the vertical refractivity gradient," *J. Atmos. Ocean. Technol.*, vol. 20, no. 6, pp. 845–855, Jun. 2003.

[28] T. R. Simons, F. R. Moore, and S. A. Gauthreaux, "Mist netting trans-gulf migrants at coastal stopover sites: The influence of spatial and temporal variability on capture data," *Stud. Avian Biol.*, vol. 29, pp. 135–143, 2004.

[29] J. E. Black and N. R. Donaldson, "Comments on 'Display of bird movements on the WSR-88D: Patterns and quantification'," *Weather Forecast.*, vol. 14, no. 6, pp. 1039–1040, Dec. 1999.

[30] K. P. Able, "The flight behaviour of individual passerine nocturnal migrants: A tracking radar study," *Animal Behav.*, vol. 25, pp. 924–935, 1977.

[31] A. Hedenström and T. Alerstam, "Climbing performance of migrating birds as a basis for estimating limits for fuel-carrying capacity and muscle work," *J. Exp. Biol.*, vol. 164, pp. 19–38, 1992.

[32] B. Bruderer, "The study of bird migration by radar—Part 1: The technical basis," *Naturwissenschaften*, vol. 94, pp. 1–8, 1997.

[33] M. Kitchen, "Representativeness errors for radiosonde observations," *Q. J. Roy. Meteorol. Soc.*, vol. 115, no. 487, pp. 673–700, Apr. 1989.

[34] K. P. Able, "Fall migration in coastal Louisiana and the evolution of migration patterns in the Gulf region," *Wilson Bull.*, vol. 84, pp. 231–242, 1972.

Jeffrey J. Buler received the B.A. degree in biology from St. Mary's College of Maryland, St. Mary's City, in 1995, the M.S. degree in wildlife from Louisiana State University, Baton Rouge, in 1999, and the Ph.D. degree in biology from The University of Southern Mississippi (USM), Hattiesburg, in 2006.

He is currently a Research Scientist with the Department of Entomology and Wildlife Ecology, University of Delaware, Newark. His research interests include wildlife–habitat relationships, landscape ecology, conservation biology, and the application of radar for studying the distributions and movements of migratory birds.

Dr. Buler was a recipient of two Mississippi Space Commerce Initiative Graduate Studies in Remote Sensing Fellowships in 2001 and 2002, a Mississippi–Alabama Sea Grant Consortium Fellowship in 2003, and the 2004 USM Innovation Award for Excellence in Graduate Research.

Robert H. Diehl received the M.S. and Ph.D. degrees in ecology from the University of Illinois, Urbana, where he used weather surveillance radars to study bird migration.

He is currently an Assistant Professor of biology with The University of Southern Mississippi, Hattiesburg. He has more than ten years of experience applying weather radar and other radio and microwave technologies to the study of animal movement.

Prof. Diehl was the recipient of a National Science Foundation Postdoctoral Fellowship in Informatics in 2003 for use of data from weather radars to guide models simulating bird habitat preferences and flight behavior.